

Influence of surface treatment on the metal dusting behavior of alloy 699 XA

Emma White¹  | Clara Schlereth¹  | Maren Lepple¹ | Heike Hattendorf²  | Benedikt Nowak² | Mathias C. Galetz¹ 

¹Materials and Corrosion Division, High Temperature Materials, DECHEMA-Forschungsinstitut, Frankfurt am Main, Germany

²Research and Development Department, VDM Metals International GmbH, Altena, Germany

Correspondence

Emma White, Materials and Corrosion Division, High Temperature Materials, DECHEMA-Forschungsinstitut, Theodor-Heuss-Allee 25, Frankfurt am Main D-60486, Germany.

Email: emma.white@dechema.de

Funding information

Horizon 2020 Research and Innovation Action, Grant/Award Number: 958192

Abstract

Metal dusting attack is a serious problem in processing industries using carbonaceous gases and high temperatures. Ni-based alloy 699 XA was recently developed as an alloy for these types of environments with high resistance against metal dusting. In this study, different surface treatments of this chromium- and aluminum-rich alloy are shown to have an important influence on the metal dusting onset behavior. It was found that surface treatments that are traditionally considered to be helpful for fatigue performance, for example, shot peening, and pickling were detrimental to the metal dusting performance of alloy 699 XA. Additionally, the shot peening surface treatment promoted Fe surface contamination, resulting in a negative impact on the metal dusting pitting resistance of the alloy. Deformation accompanied by apparent BCC α -Cr precipitation in the bulk microstructure, but a comparison with cold-rolled materials shows that the surface treatment dominates the metal dusting resistance.

KEYWORDS

metal dusting, Ni-based alloy, oxide former, plastic deformation, shot peening, surface treatment

1 | INTRODUCTION

In atmospheres containing carbonaceous gases at temperatures between 400°C and 800°C, metal dusting can be observed as a high-temperature corrosion process that is catastrophic due to the uncertainty in pit initiation time and rapid pit growth.^[1] These types of conditions are widely present in methanol plants, iron ore reduction, and synthesis gas production.^[1–4] Metal dusting of austenitic Ni-based alloys is characterized by carbon deposition onto the metal, due to the high carbon activity of the gas, which subsequently causes carbon diffusion and supersaturation in the subsurface zone. With carbon supersaturation, graphite

crystallization is favorable at the surface and grain boundaries, which then, due to volume expansion, disintegrates the metal, forming large quantities of coke with carbide, oxide, and metal nanoparticles.^[5–7] Highly alloyed materials (with Sn and Cu for catalytic inhibition; Al, Cr, and Si for surface oxide formation), coatings, and surface treatments can delay the onset or even prevent metal dusting.^[8–16] An alumina, chromia, or silica dense, continuous oxide scale, with high enough content of the oxide former in the subsurface zone to reheat any defects/cracks, will considerably improve the resistance to metal dusting.^[17] Alloy 699 XA is a Ni-based alloy with ~30 wt.% Cr and 2 wt.% Al, sufficient alloying additions to be superior to alloy

This is an open access article under the terms of the Creative Commons Attribution License, which permits use, distribution and reproduction in any medium, provided the original work is properly cited.

© 2022 DECHEMA Forschungsinstitut and VDM Metas International GmbH. *Materials and Corrosion* published by Wiley-VCH GmbH.

602 CA and alloy 690 in metal dusting environments.^[18–20] In a previous study of metal dusting attack (600°C, 20 bar, 37% CO-9% H₂O-7% CO₂-46 vol.% H₂) on a weld joint of alloy 699 XA, a protective outer chromia layer and an inner continuous alumina scale were obtained on the surface of the fine-grained regions, while a thicker outer chromia layer with an inner alumina scale formed over the coarse-grained areas.^[19] This thicker chromia surface scale had a thinner and less uniform underlying alumina layer than what was observed in the fine-grained regions, which resulted in diminished metal dusting resistance.^[19]

Surface treatments of mill grinding, shot peening, pickling, and brushing can all affect the surface roughness, grain size, and defect concentration, which changes the metal dusting behavior of any base alloy.^[21–24] Improvements in the resistance to metal dusting attack are observed when these treatments promote oxide scale formation. Maier et al., in their study of Fe–Cr–Ni alloys, compared ground versus polish-etched sample surfaces and found the residual surface working from grinding to increase the number of fast diffusion paths, subsequently improving the nucleation and growth of a protective surface oxide and thus the metal dusting resistance.^[25] For the previous 699 XA weld study, initial observations of ground side surfaces had higher metal dusting resistance than the as-welded surface, motivating further investigations.^[19] In this study, Ni-based alloy 699 XA with various surface treatments (mill grinding, shot peening, and mild pickling) was subjected to a harsh metal dusting environment to evaluate the optimum surface finish for protective behavior. In addition, to distinguish surface from subsurface deformation effects, the influence of cold rolling of up to 50% bulk deformation on the metal dusting attack was also studied and compared.

2 | EXPERIMENTAL PROCEDURE

2.1 | Alloy and surface treatments

VDM® Alloy 699 XA was melted in an electric furnace and electro-slag remelted (ESR). The chemical composition is shown in Table 1. Plates with thicknesses of 16 mm and 25 mm were produced by a hot-rolling process with a subsequent solution annealing. Afterward, the surfaces of the plates were ground in the mill to remove the oxide scale. Samples 1–3 were taken from the 16 mm plate for the investigation of different surface treatments and samples 4–7 from the 25 mm plate for the investigations with different cold rolling levels (0%, 2%, 10%, 50%), as illustrated in Table 2. A piece of the 16 mm plate was included as-ground by the mill for reference (sample number 1). For samples numbered 2 and 3, the surface was shot-peened with steel shot after the grinding

TABLE 1 Chemical composition (wt.%) of the alloy 699 XA

C	Cr	Ni	Mn	Si	Ti	Nb	Fe	Al	Zr	Other
0.02	29.5	68.0	<0.01	0.1	0.01	0.1	0.1	2.1	0.03	<0.1

TABLE 2 Sample list with an explanation of the prepared state

Sample no.	Preparation
1	Mill ground (no additional preparation)
2	Shot-peened
3	Shot-peened + mild pickling
4	0% cold rolled, P500 grit polish
5	2% cold rolled, P500 grit polish
6	10% cold rolled, P500 grit polish
7	50% cold rolled, P500 grit polish

during production. For sample number 3, an additional mild pickling process (25% HNO₃ at 50°C for 1 min) was applied after shot-peening. After the preparations described above, the 4–5 mm thick test coupons were machined by wire-cutting to the final dimensions of 20 × 10 mm as determined using an electronic caliper, but leaving the specially treated main surfaces untouched. The machined side and back surfaces were polished to a P500 grit finish using SiC paper for reference. Exposures under the same conditions were previously reported, which compare the metal dusting performance of 602CA and 699 XA in the ground surface condition and thus no additional reference alloy is included in this study.^[26]

To study the relationship between different cold rolling levels and sensitivity to metal dusting attack, three samples of the 699 XA 25 mm plate were cold rolled to 2%, 10%, and 50% deformation, as shown in Table 2. Sample number 4 was the reference without cold rolling. All surfaces of the rolled samples were polished to a P500 grit finish using SiC paper before exposure to the metal dusting environment.

2.2 | Metal dusting exposure and characterization

Metal dusting exposure tests were conducted in a metal dusting test rig for elevated pressure tests, consisting of a tube furnace with flowing atmosphere control. The various samples were placed in separate alumina crucibles in a horizontal arrangement (tube material: Centralloy® ET 45 Micro). A more detailed description of the testing equipment was previously given.^[27] The tube furnace was purged with argon (<2 ppm oxygen, 4 L/h)

overnight, the furnace temperature was raised to 620°C, and the defined atmosphere of 47% CO-47% H₂-2% H₂O-4 vol.% CO₂ was released into the furnace and then pressurized to 19 bar. The gas velocity was set to 1.03 cm/min at the samples. The carbon activity was calculated individually for the synthesis gas reaction and Boudouard reactions.

$$a_{C(1)} = K_{(1)} \frac{p_{CO} p_{H_2}}{p_{H_2O}}, \quad (1)$$

$$a_{C(2)} = K_{(2)} \frac{p_{CO}^2}{p_{CO_2}}, \quad (2)$$

where $K_{(1)}$ and $K_{(2)}$ are the equilibrium constants for the synthesis gas and Boudouard reactions, respectively. The carbon activity of the unreacted gas mixture of the listed atmosphere is 634 according to the synthesis gas reaction and 663 according to Boudouard reaction calculations.

The specimens were exposed for two periods of 240 h at 19 bar and 620°C. To end the tests, the pressure was decreased, the furnace was flushed with argon (<2 ppm oxygen, 4 L/h), and allowed to cool to room temperature simultaneously. The resulting samples were cleaned in an ultrasonic bath with water and ethanol after each exposure. Cross-sections were prepared using conventional metallographic methods including galvanic Ni-plating, grinding up to P1200 grit SiC paper, and polishing down to 1 μm using diamond suspensions. Some cross-sections were etched using the V2A etchant at 50°C to better observe the alloy microstructure underneath the oxide scales. Elemental compositions were performed on an electron probe microanalysis (EPMA) Jeol JXA-8100 instrument equipped with a W cathode. Five-spot measurements of the unexposed surfaces were taken on each sample at 15 kV, 30 nA probe current, and a probe diameter of less than 1 μm and then were averaged.

3 | RESULTS

For comparison, macroimages of the surface-treated and P500-polished sides of each sample, after 2 × 240 h of exposure in the above-described conditions, are included in Figure 1, demonstrating the behavioral difference is solely related to the surface treatment. Cross-sections of the exposed surface treatments without (a) and with etching (b) are shown in Figure 2. Representative metal dusting pits are characterized by coke, a carbon-enriched zone, and a carburized zone. Carbon is dissolved in the matrix in the carburized zone and is visible after etching as demonstrated for the mill ground + shot peened + mild-pickling sample in Figure 2b. A previous metal dusting study on alloy 699

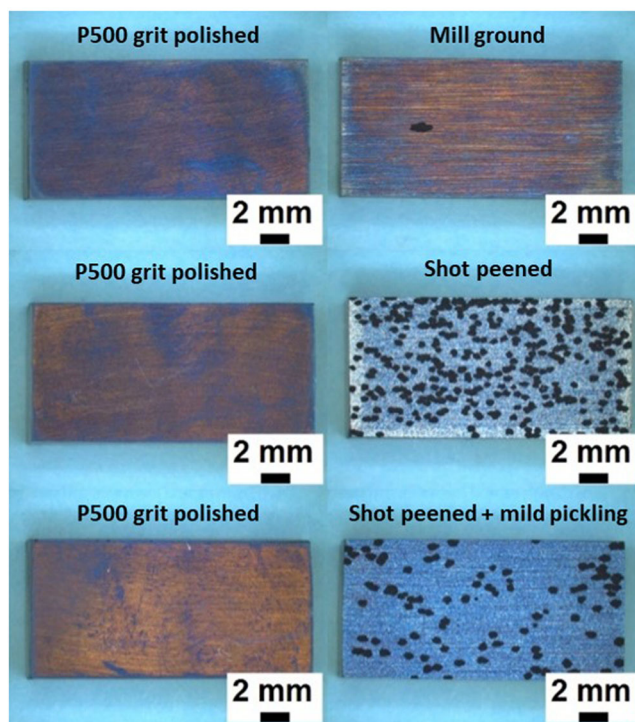


FIGURE 1 Light microscope images of the metal dusting of the surface-treated versus P500 grit polished surfaces. [Color figure can be viewed at wileyonlinelibrary.com]

XA showed these same representative features and that the carbon-enriched zone contains lamellar Cr₃C₂ precipitates in a Cr-depleted, Ni-rich matrix.^[19]

All cold-rolled samples of alloy 699 XA showed fair metal dusting resistance up to 2 × 240 h as shown by the macroimages in Figure 3, with only minor pit formation. The few pits that formed were only on the deformed samples, and the samples from 2% to 50% deformation showed a similar amount of pitting, with no apparent effect of the extent of deformation on metal dusting pit formation. Figure 4 gives the optical cross-sections of the cold-rolled samples (0%, 2%, 10%, and 50%), through a pit if available, both without (a) and with (b) etching to highlight the microstructural features. The number of twin boundaries clearly increases with increasing percent of deformation. Additionally, as deformation increased (especially 50% cold-rolled), it was accompanied by apparent fine BCC α-Cr precipitation throughout the bulk of the material.

4 | DISCUSSION

In the previous study of a 699 XA weld, it was well established that this alloy forms an outer chromia layer and an inner alumina layer at 620°C in low oxygen partial pressure (~10⁻⁶ atm) environments.^[19] A similar

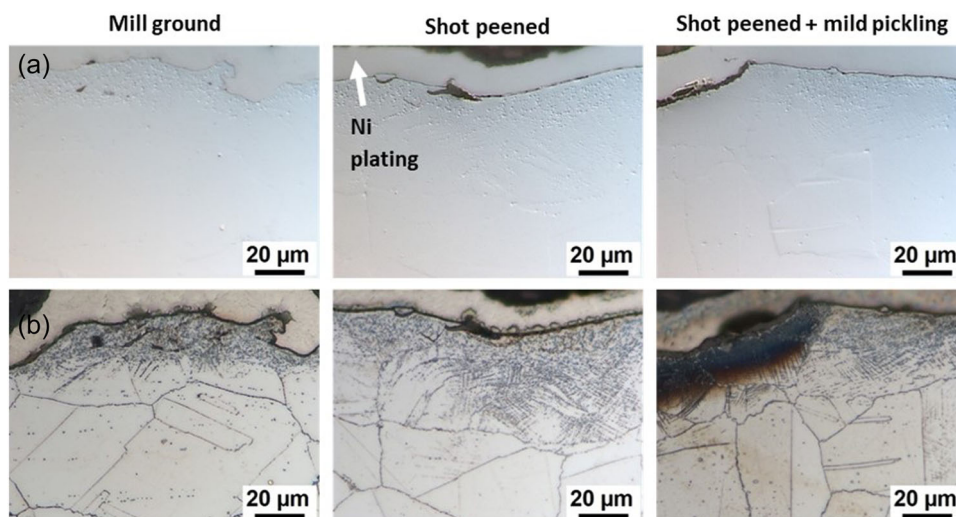


FIGURE 2 Base metal alloy 699 XA after metal dusting exposure; cross-sections (a) without and (b) with etching. All samples have galvanic Ni-plating for cross-sectional preparation (labeled in the (a) shot-peened image). [Color figure can be viewed at [wileyonlinelibrary.com](https://onlinelibrary.wiley.com/doi/10.1002/maco.202213380)]

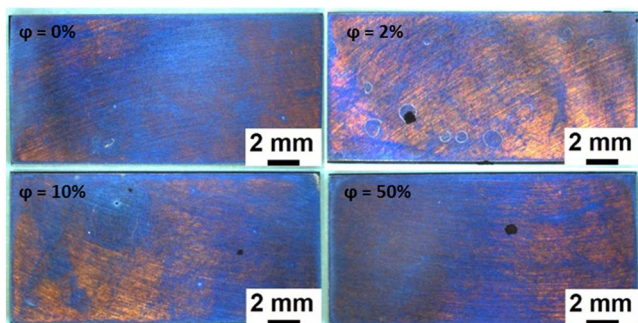


FIGURE 3 Light microscope images of cold-rolled alloy 699 XA specimens after metal dusting exposure. Darker, black regions are indicative of pit formation during exposure. [Color figure can be viewed at [wileyonlinelibrary.com](https://onlinelibrary.wiley.com/doi/10.1002/maco.202213380)]

oxide scale is expected to have formed in these experiments; however, these thin (<50 nm) layers are below the resolution of the investigation techniques in this study and therefore Al and Cr are grouped together in the following discussion.

It is clear that all cases of additional surface treatments, beyond mill grinding, resulted in a higher density of similarly sized metal dusting pits (Figure 1). Shot-peened surfaces demonstrated the worst performance, whereas subsequent mild pickling appeared to mitigate pit formation slightly. Classically, shot peening is described as improving metal dusting performance by increasing the surface dislocation density and thus increasing Al and Cr outward diffusion for improving the passivation and re-healing of the oxide layer.^[21,22,28] Commonly, any type of near-surface deformation is advertised as improving metal dusting resistance.^[14,29–31] However, this neglects the contamination potential from post-processing, such as the transfer of the

shot material to the substrate, which could counteract the benefits that were sought.^[32] In the current study, the samples were shot-peened with steel balls, which increased the Fe content of the surface zone as evidenced by the EPMA measurements included in Figure 5. Fe in the oxide layer promotes C deposition,^[33–35] and as seen in these results, lowers the metal dusting resistance of the material. Subsequent pickling of the sample removed some of the surface contamination so the performance was slightly improved, but not returned fully to the base material (mill ground) level, as pickling also removes the oxide scale and lowers the Al and Cr availability in the near-surface zone (see Figure 5).^[21,22,24] Still the Fe and C levels, even after pickling, remain much higher than in the original mill ground condition.

Grinding causes the near-surface grain size to be much smaller than the bulk and increases the dislocation density.^[36,37] These boundaries and dislocations form easy diffusion paths for Al and Cr to rapidly form a protective oxide scale. Grinding does not significantly affect C inward diffusion as bulk diffusion at 600°C is rapid due to the large interstitial spacing in the FCC lattice.^[38] The grain size near the surface and the availability of grain boundaries for Cr diffusion are decisive for corrosion resistance, as was demonstrated by transmission electron microscopy studies.^[37,39]

The cold rolling influence on metal dusting further indicated that only the near-surface deformation affects Al/Cr availability in this system. All surfaces of these cold-rolled samples were polished with a P500 grit. The severely deformed subsurface zone from polishing produces defect densities that are more critical to the flux of Cr to the surface than the bulk of the material.^[39] Gheno et al.,

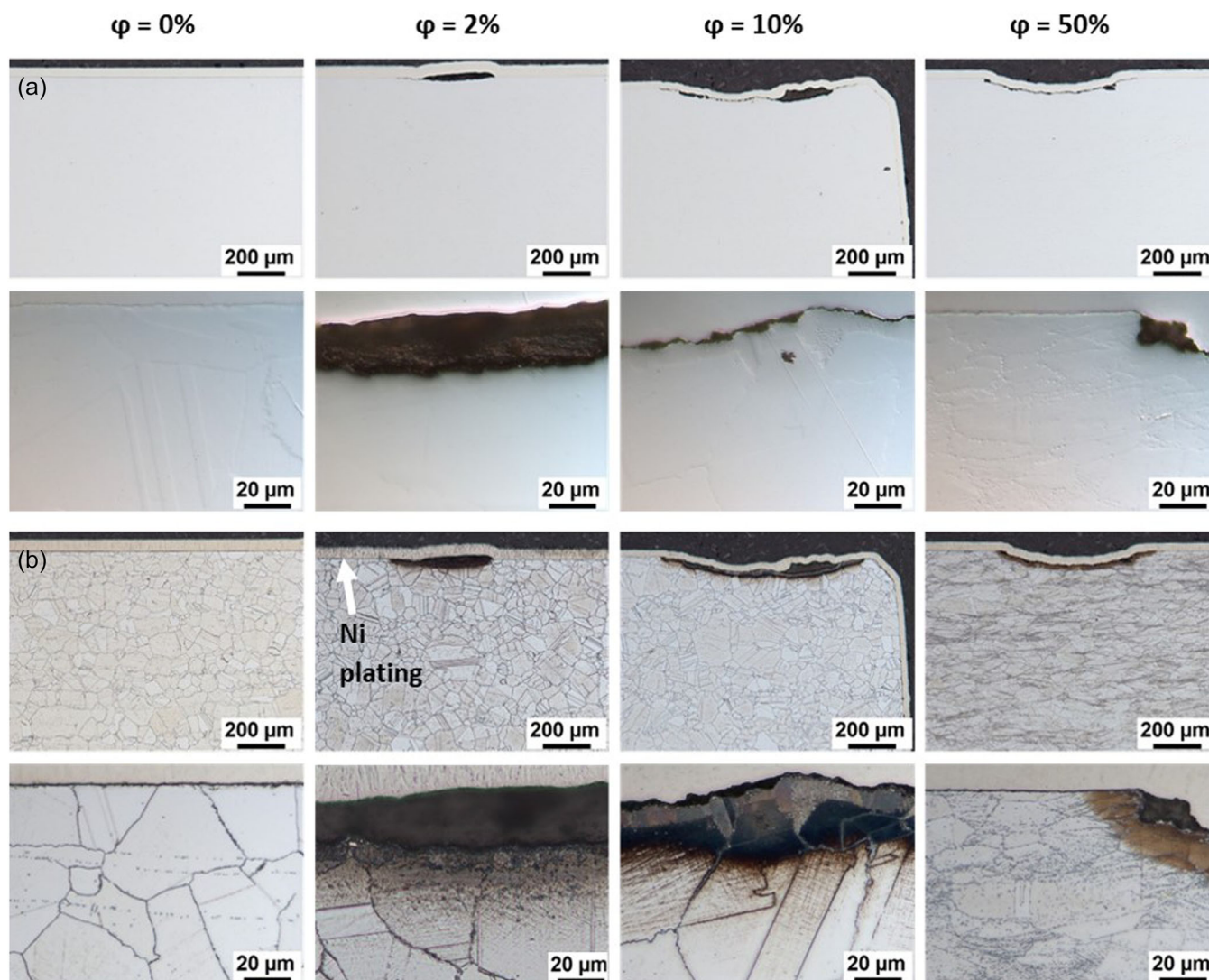


FIGURE 4 Optical cross-sectional images of the cold-rolled alloy 699 XA and pits after metal dusting exposure: (a) without etching, (b) with etching to highlight grain boundaries and carburized zones. The top layer on all samples is galvanic Ni-plating for cross-sectional preparation (labeled in the (b) 2% image) and is especially clear over the pits in the 2%, 10%, and 50% cold-rolled samples. [Color figure can be viewed at wileyonlinelibrary.com]

studied the oxidation (550°C in air) of a cold-worked (50%–90%) and annealed Ni-30 wt.%Cr alloy where they concluded that accelerated grain boundary diffusion in the metal was the predominant mechanism for oxide scale formation, over dislocation diffusion, and bulk diffusion at the investigated temperature, which is not far from the 620°C of this study.^[39] Their samples had shallow deformation zones of 30–300 nm from polishing and grinding, which were of similar procedures to this study. The present results suggest that grain boundary Cr diffusion was the main contributing factor to the chromia scale formation. Dislocation contributions to Al and Cr diffusion were not as significant since the metal dusting behavior of all cold-rolled samples was similar, despite different dislocation densities in

the bulk material from varying levels of cold work. The metal dusting performance was also similar across the cold-rolled samples, despite varying levels of BCC α -Cr precipitation, which highlights the role of the inner alumina scale formation. In these intermediate temperature ranges with severely deformed microstructures, there can be difficulty in understanding the corrosion mechanisms due to uniformity and evolution during recovery, recrystallization, and grain growth throughout the experiments. However, these results show that only the deformation close to the surface is decisive, due to the rather low temperatures for scale formation, which limits the diffusion and depletion of oxide formers (Al and Cr) to the first few microns below the surface of the metal.

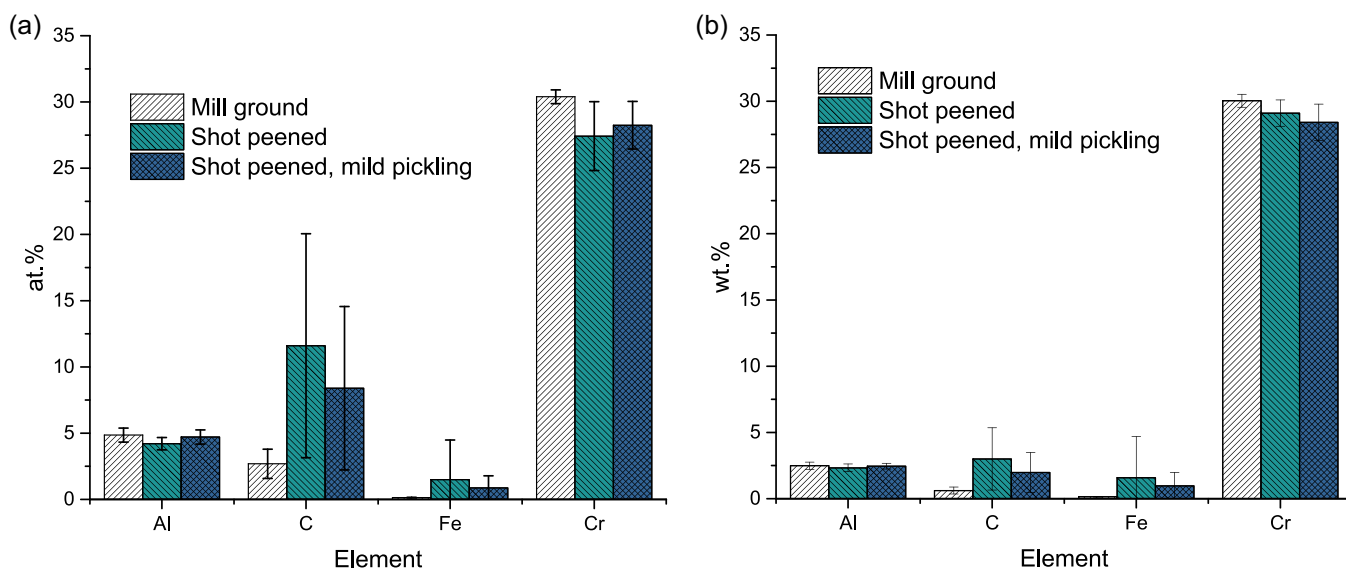


FIGURE 5 EPMA measurements of Al, Cr, Mn, and Fe for different surface treatments, (a) at.% and (b) wt.%. Error bars are \pm the standard deviation of five measurements within the same overall areas. [Color figure can be viewed at wileyonlinelibrary.com]

5 | CONCLUSION

This study investigated the metal dusting behavior of Alloy 699 XA with different surface treatments in a 47% CO-47% H₂-2% H₂O-4 vol.% CO₂ atmosphere at 620°C and 19 bar. The findings of the study can be summarized as follows:

- The mill ground condition was the most resistant to metal dusting due to the high level of near-surface deformation, which allowed fast Al and Cr diffusion.
- Shot peening was detrimental to the metal dusting performance due to the transfer of the steel shot material to the alloy surface and subsequent contamination with Fe and C, which reduced the metal dusting resistance.
- Mild pickling after shot peening removed some of the surface contamination, but also the oxide layer, which significantly affected the Cr content and thus still had worse metal dusting behavior than the original mill ground condition.

Additionally, cold-worked specimens of the same composition confirmed the criticality of the level of deformation in the near-surface zone to the oxide layer formation and thus to the metal dusting resistance. The varying levels of cold-work from 0% to 50% did not significantly change the metal dusting behavior despite the increasing level of dislocations in the bulk material, affirming that the near-surface grain boundary diffusion was the most significant contributor to the Al and Cr flux and metal dusting resistance.

Overall the surface treatment influence on the metal dusting resistance of Alloy 699 XA was observed to be similar to other structural materials with respect to deformation improving the density of fast diffusion paths, which leads to improved oxide scale nucleation and growth.^[19,25] In this particular case, shot peening was not beneficial, as it not only increased the level of near-surface deformation, but also contaminated the alloy surface, which had a stronger impact and resulted in an increased metal dusting attack.

ACKNOWLEDGMENTS

The authors would like to acknowledge VDM Metals International GmbH for supporting this project. The authors would like to thank Mathias Röhrig for preparation of the samples and assistance with the exposure tests. The authors would also like to thank Ellen Berghof-Hasselbächer for preparation of the cross-sections and optical microscopy imaging and Dr. Gerald Schmidt for conducting the EPMA measurements. This project has received funding from the European Union's Horizon 2020 Research and Innovation Programme under grant agreement No 958192.

DATA AVAILABILITY STATEMENT

The data that support the findings of this study are available from the corresponding author upon request.

ORCID

Emma White  <http://orcid.org/0000-0002-0246-6256>

Clara Schlereth  <http://orcid.org/0000-0002-5770-782X>

Heike Hattendorf  <http://orcid.org/0000-0002-8609-0910>

Mathias C. Galetz  <http://orcid.org/0000-0001-6847-2053>

REFERENCES

- [1] C. M. Schillmoller, *Chem. Eng.* **1986**, *93*, 83.
- [2] H. J. Grabke, M. Spiegel, *Mater. Corros.* **2003**, *54*, 799.
- [3] E. Slevolden, J. Z. Albertsen, U. Finck, in *Proceedings of Corrosion 2011*, NACE, Houston, Texas **2011**.
- [4] J. J. Hoffman, M. Lin, W. R. Watkins, S. W. Dean, in *Proceedings of Corrosion 2009*, NACE, Houston, Texas **2009**.
- [5] H. J. Grabke, in *Corrosion by carbon and nitrogen: Metal dusting, carburisation and nitridation (EFC 41)* (Eds: H. J. Grabke, M. Schütze), Woodhead Publishing, Cambridge **2007**, pp. 1.
- [6] D. J. Young, J. Zhang, C. Geers, M. Schütze, *Mater. Corros.* **2011**, *62*, 7.
- [7] J. Zhang, D. J. Young, *Corros. Sci.* **2007**, *49*, 1496.
- [8] C. Geers, M. Schütze, *ECS Trans.* **2009**, *25*, 71.
- [9] S. Madloch, M. C. Galetz, C. Geers, M. Schütze, *Surf. Coat. Technol.* **2016**, *299*, 29.
- [10] C. G. M. Hermse, H. van Wortel, in *Proceedings of Corrosion 2009*, NACE, Houston, Texas **2009**.
- [11] Y. Nishiyama, K. Moriguchi, N. Otsuka, T. Kudo, *Mater. Corros.* **2005**, *56*, 806.
- [12] S. B. Parks, C. M. Schillmoller, *Hydrocarbon Process.* **1997**, *October*, 93–98.
- [13] B. A. Baker, G. D. Smith, in *International Workshop on Metal Dusting, ANL, Argonne, IL, September 26–28, 2001*, Special Metals Technical Paper, Argonne, IL **2001**.
- [14] A. Agüero, M. Gutiérrez, L. Korcakova, T. Nguyen, B. Hinnemann, S. Saadi, *Oxid. Met.* **2011**, *76*, 23.
- [15] I. Wolf, H. J. Grabke, *Solid State Commun.* **1985**, *54*, 5.
- [16] K. Natesan, Z. Zeng, in *Proceedings of Corrosion 2005*, NACE, Houston, Texas **2005**.
- [17] M. Schütze, in *Reference Module in Materials Science and Materials Engineering* (Ed: S. Hashmi), Elsevier, Amsterdam **2016**, pp. 1.
- [18] W.-T. Chen, B. Li, B. Gleeson, M. C. Galetz, H. Hattendorf, in *Proceedings of Corrosion 2019*, NACE, Houston, Texas **2019**.
- [19] H. Hattendorf, A. López, J. Kloewer, in *Proceedings of Corrosion 2018*, NACE, Houston, Texas **2018**.
- [20] A. Fabas, D. Monceau, S. Doublet, A. Rouaix-Vande Put, *Corros. Sci.* **2015**, *98*, 592.
- [21] H. J. Grabke, *Mater. Corros.* **2003**, *54*, 736.
- [22] H. J. Grabke, E. M. Müller-Lorenz, M. Zinke, *Mater. Corros.* **2003**, *54*, 785.
- [23] D. Röhner, M. Schütze, T. Weber, in *Corrosion 2007 Conference & Expo*, NACE, Nashville **2007**, pp. 7417.
- [24] C. G. M. Hermse, H. van Wortel, in *Proceedings of Eurocorr 2008, Edinburgh*, DECHEMA e.V, Frankfurt am Main **2008**.
- [25] M. Maier, J. F. Norton, P. Puscheck, *Mater High Temp* **2000**, *17*, 347.
- [26] C. Schlereth, C. Oskay, H. Hattendorf, B. Nowak, M. C. Galetz, *Mater. Corros.* **2022**, *73*, 1346.
- [27] S. Madloch, A. Soleimani-Dorcheh, M. C. Galetz, *Oxid. Met.* **2018**, *89*, 483.
- [28] H. J. Grabke, *Mater. Corros.* **1998**, *49*, 303.
- [29] H. J. Grabke, R. Krajak, E. M. Müller-Lorenz, *Mater. Corros.* **1993**, *44*, 89.
- [30] J. C. Nava Paz, H. J. Grabke, *Oxid. Met.* **1993**, *39*, 437.
- [31] X. Guo, P. E. Vullum, H. J. Venvik, *Corros. Sci.* **2021**, *190*, 109702.
- [32] S. Bagherifard, *Adv. Eng. Mater.* **2019**, *21*, 1801140.
- [33] Z. Zeng, K. Natesan, *Oxid. Met.* **2006**, *66*, 1.
- [34] H. Hattendorf, C. G. Hermse, R. M. IJzerman, *Mater. Corros.* **2019**, *70*, 1385.
- [35] B. Li, B. Gleeson, W.-T. Chen, H. Hattendorf, in *Proceedings of Corrosion 2020*, NACE, Houston, Texas **2020**.
- [36] H. J. Grabke, E. M. Müller-Lorenz, M. Zinke, in *Corrosion by Carbon and Nitrogen: Metal Dusting, Carburisation and Nitridation (EFC 41)* (Eds: H. J. Grabke, M. Schütze), Woodhead Publishing, Cambridge **2007**, pp. 59.
- [37] H. J. Grabke, E. M. Müller-Lorenz, S. Strauss, E. Pippel, J. Woltersdorf, *Oxid. Met.* **1998**, *50*, 241.
- [38] J. Z. Albertsen, O. Grong, J. C. Walmsley, R. H. Mathiesen, W. van Beek, *Metall. Mater. Trans. A* **2008**, *39*, 1258.
- [39] T. Gheno, C. Desgranges, L. Martinelli, *Corros. Sci.* **2020**, *173*, 108805.

How to cite this article: E. White, C. Schlereth, M. Lepple, H. Hattendorf, B. Nowak, M. C. Galetz, *Mater. Corros.* **2023**;74:190–196.

<https://doi.org/10.1002/maco.202213380>